

Communication-Efficient Personalized Distributed Learning with Data and Node Heterogeneity

Zhuojun Tian, *Member, IEEE*, Zhaoyang Zhang, *Senior Member, IEEE*, Yiwei Li, *Senior Member, IEEE*, and Mehdi Bennis, *Fellow, IEEE*

Abstract—To jointly tackle the challenges of data and node heterogeneity in decentralized learning, we propose a distributed strong lottery ticket hypothesis (DSLTH), based on which a communication-efficient personalized learning algorithm is developed. In the proposed method, each local model is represented as the Hadamard product of global real-valued parameters and a personalized binary mask for pruning. The local model is learned by updating and fusing the personalized binary masks while the real-valued parameters are fixed among different agents. To further reduce the complexity of hardware implementation, we incorporate a group sparse regularization term in the loss function, enabling the learned local model to achieve structured sparsity. Then, a binary mask aggregation algorithm is designed by introducing an intermediate aggregation tensor and adding a personalized fine-tuning step in each iteration, which constrains model updates towards the local data distribution. The proposed method effectively leverages the relativity among agents while meeting personalized requirements in heterogeneous node conditions. We also provide a theoretical proof for the DSLTH, establishing it as the foundation of the proposed method. Numerical simulations confirm the validity of the DSLTH and demonstrate the effectiveness of the proposed algorithm.

Index Terms—Distributed learning, personalized learning, data and node heterogeneity, communication efficiency.

I. INTRODUCTION

As one of the most promising applications in 6G era, Artificial Intelligence of Things (AIoT) combines the artificial intelligence technologies with the Internet of Things (IoT) infrastructure, resembling the transformation from “connected things” to “connected intelligence”. In AIoT, edge learning

This work was supported in part by National Natural Science Foundation of China under Grants 62394292 and U20A20158, Ministry of Industry and Information Technology under Grant TC220H07E, Zhejiang Provincial Key R&D Program under Grant 2023C01021, the Fundamental Research Funds for the Central Universities No. 226-2024-00069, and the EU-SNS 6G CENTRIC Project.

Z. Tian (email: dankotian@zju.edu.cn) was with the College of Information Science and Electronic Engineering, Zhejiang University, Hangzhou 310027, China and now is with the Center for Wireless Communications, University of Oulu, Oulu 90014, Finland.

Z. Zhang (Corresponding Author, email: ning_ming@zju.edu.cn) is with the College of Information Science and Electronic Engineering, Zhejiang University, Hangzhou 310027, China, and with the State Key Laboratory of Industrial Control Technology, Hangzhou 310027, China, and also with Zhejiang Provincial Key Laboratory of Multimodal Communication Networks and Intelligent Information Processing, Hangzhou 310027, China.

Y. Li (e-mail: lywei0306@foxmail.com) is with Fujian Key Laboratory of Communication Network and Information Processing, Xiamen University of Technology, Xiamen 361024, China.

M. Bennis (e-mail: mehdi.bennis@oulu.fi) is with the Center for Wireless Communications, University of Oulu, Oulu 90014, Finland.

The code for the paper is available on <https://github.com/ZhuoJTian/MCE-PL>.

has been envisioned as the key enabler to embed model training and inference into network, utilizing the computation and communication capability of devices. In conventional edge learning procedures, each agent has access to its own training data and cooperates with others to obtain a common global model [1]. However, due to different geographical locations or various users to serve, agents often have partial views of global information [2], leading to heterogeneous data distributions. Under such non-identically and independently distributed (non-i.i.d.) conditions, the consensus model typically performs poorly on locally accessible data, motivating researchers to explore personalized learning among agents [3].

Recently, in the increasingly complex AIoT application scenarios, agents tend to exhibit diverse system capabilities, ranging from servers with high computational power and large storage capacity to mobile phones or sensors with limited capabilities. In this sense, the concept of personalization needs to be expanded to address the challenge of node heterogeneity, where each agent’s personalized model should adapt to local system characteristics. This motivates us to jointly consider the data (statistical) and node (system) heterogeneity in AIoT system by developing personalized models for each agent. Moreover, the frequent communication in the training process brings high communication costs, which is a major challenge in AIoT system. Therefore, our goal is to design a communication-efficient personalized algorithm that accounts for both node and data heterogeneity.

In this work, we investigate decentralized communication networks. Different from the popular Federated Learning (FL) framework, decentralized learning does not rely on a central node to collect and process all agents’ messages, thereby alleviating the heavy communication burden on the center node and enhancing robustness against nodes’ failure. In decentralized learning, each agent typically updates its local model and then shares the updated model with neighboring nodes for aggregation. The standard aggregation methods, such as averaging or weighted averaging used in decentralized stochastic gradient descent [4], often perform poorly in non-i.i.d. conditions. Therefore, a specialized aggregation design is necessary to effectively leverage the relationships among agents in this non-i.i.d. and heterogeneous system.

A. Related Works

Recently, many works have focused on addressing the non-i.i.d. challenges in FL by designing personalized learning algorithms [5–9]. Specifically, meta-learning methods have

been applied in FL [5] to enable personalized training. The work [6] clustered the agents and used the graph convolution networks to share knowledge across different clusters. More recently, the node heterogeneity problem in FL has gained attention, particularly where clients have distinct capabilities [12]. The existing methods can generally be classified into three categories: split-learning based methods [10, 11], sub-model training methods [12–14, 16, 17] and the methods based on factorization [18–20]. The work [12] questioned the assumption of the same global model and proposed the HeteroFL framework, where local model parameters in each client form a subset of the global model, and aggregation is performed through partial averaging. The work [13] introduced ordered pruning to extract and train different submodels for different clients. Other works [18–20] focused on compressing large global models into small models by low-rank factorization and assign the small models to different clients based on their capabilities. In all these methods, a central server is responsible for maintaining the large global model and handling tasks such as model partition, compression and factorization. However, in the decentralized framework, there is no central processor to perform these tasks, making it challenging to directly apply these methods to decentralized learning.

On the other hand, there have been fewer works addressing personalization in decentralized learning [3, 21–23]. The work [21] constructed a collaborative graph to represent the correlation among the tasks of different agents. During training, both the collaborative graph and the local models are alternatively learned to obtain the personalized model for each agent, which however highly increases the computation and communication cost. The methods in [3] and [22] utilize partially shared local models. The work [3] employed a graph attention mechanism to jointly learn aggregation weights, while the work [22] introduced a topology reconstruction algorithm to reduce the communication bandwidth and accelerate the training process. Nevertheless, the above works only focused on statistical personalization, where the personalized models share a common neural network architecture, without addressing node heterogeneity. To resolve this issue, the work [24] proposed the Dis-PFL protocol employing personalized sparse masks, where the active parameters and local masks are transmitted while those intersection weights are averaged. The work [25] proposed dynamically adjusting batch sizes to enhance data parallelization and exchanging prioritized gradients to reduce communication overhead. Meanwhile, the work [26] addressed the long-tail effects caused by node heterogeneity, introducing a hierarchical synchronization procedure to minimize latency.

In distributed learning, the large number of transmitted model parameters and the continuous iterations lead to high communication costs in practical wireless communication systems. Consequently, there have been extensive works aiming to reduce the communication cost through resource allocation, over-the-air computation [27], accelerating convergence [28], and minimizing communication cost per iteration [29–32]. In the latter approach, some works have explored client selection while others have focused on model compression by model sparsification, gradient compression or parameter quantization.

The authors in [31] proposed a first-order computationally efficient distributed optimization algorithm, which shows stability in time-varying networks, and they extend the methods in [32] for log-scale quantized data exchange. These techniques can be generally applied in both FL and decentralized frameworks. Additionally, the authors in [34] introduced the communication-efficient FL techniques using compression, which meanwhile solves privacy concerns against poisoning and inference attacks through secure aggregation. The secure blockchain-enabled algorithm in [34] further utilizes blockchain-enabled steps to address the privacy issue.

The work [33] proposed to reduce the communication costs by utilizing the lottery ticket hypothesis, where the sparse binary masks are learned and transmitted among agents. The masks from different clients are partially aggregated, where overlapping entries across the binary masks are aggregated while non-overlapping entries remain unchanged. This approach effectively learns personalized models for each agent while significantly reducing communication costs. Similar to the procedure in [33], many works [15–17, 24] have applied the lottery ticket hypothesis as a pruning technique to tackle the heterogeneity in distributed learning. The authors in [15] proposed LotteryFL for data heterogeneity, where clients prune their local model based on the received global model. Concerning the scalability and stragglers problem in LotteryFL, another algorithm is designed in [16] exploiting the downlink broadcast. The authors in [17] further considered the system heterogeneity and designed a two-stage pruning method on both client and server sides, where the model size is adapted to reduce both communication and computation overhead. However, it still requires the central server to prune all clients. To provide a good solution for decentralized heterogeneity, the authors in [24] proposed Dis-PFL to save the communication and computation cost. However, in all of the above algorithms, the real-valued model parameters are transmitted, leading to high communication cost even with sparse masks.

B. Contributions

To further reduce communication costs in decentralized learning framework that simultaneously considers data and node heterogeneity, we adopt the core idea from [33] to learn personalized sparse binary tensors. We propose and verify the distributed strong lottery ticket hypothesis (DSLTH), serving as the theoretical foundation for this approach. In [33], the initialization of the real-valued mask from the aggregated binary tensor is challenging. Moreover, the model aggregation based on overlapping masks is unsuitable for system heterogeneous scenarios, as the aggregated mask tends to become sparser, limiting the utilization of the diverse capabilities of agents. To solve this issue, we design a novel aggregation algorithm for the binary tensors. Note that our work differs from [24], where the proposed method only transmits binary masks among agents and the personalized masks are collaboratively learned. On the contrary, Dis-PFL in [24] transmits both real-valued parameters and masks and updates both of them. Compared with the methods based on quantization [32], the mask is naturally binary, reducing the communication cost without quantization.

Specifically, we integrate the information from neighboring binary masks into the local real-valued mask tensor through an intermediate aggregation tensor, where the influence of the binary information is adaptively modulated by our specialized design. Moreover, we incorporate a personalized fine-tuning step in each iteration to ensure that the learned personalized model aligns with the local data distribution. Unlike methods that fuse binary masks through intersection, our algorithm aggregates binary mask information directly into real-valued tensors, offering greater flexibility for heterogeneous conditions. Our key contributions can be summarized as follows:

- We propose DSLTH for heterogeneous distributed learning systems, laying the foundation of the algorithm development. By introducing an intermediate aggregation tensor, the binary masks from neighboring nodes can be fused into local real-valued mask tensor. Moreover, we incorporate a personalized fine-tuning step in the update process, ensuring that the personalized model moves towards local data distribution.
- This work presents a novel framework for decentralized learning that simultaneously addresses both data and node heterogeneity by tailoring personalized models for individual agents. Additionally, based on the proposed DSLTH, the communication cost is significantly reduced during the training process while guaranteeing the learning performance, making this approach highly applicable for future AIoT systems.
- The distributed strong lottery ticket hypothesis is theoretically proved for non-i.i.d. data distribution. We further verify the hypothesis in node heterogeneity through testing experiments. The effectiveness and communication-efficiency of the proposed algorithm are demonstrated through experimental results, where the agents collaboratively learn their personalized and heterogeneous models with minimal communication cost.

The rest of this article is organized as follows: Section II describes the system model and the model learning method based on binary masks. In Section III-A, we propose the distributed strong lottery ticket hypothesis. Then in Section III-B, we introduce the group sparsity regularization term added in the loss function and then describe the rule to obtain the binary mask tensor. Then in Section III-C, we develop the aggregation and updating procedure named as MCE-PL for communication-efficient personalized learning. Section IV provides the theoretical proof for the proposed DSLTH, providing the theoretical foundation of the proposed method. Simulation results are represented in Section V, followed by the conclusion in Section VI.

II. PRELIMINARY

A. System Model

Consider a multi-agent decentralized communication network as shown in Fig. 1, which can be represented by an undirected graph $\mathcal{G} = (\mathcal{V}, \mathcal{E})$. The communication network is assumed to be connected and static over the training process. In \mathcal{G} , $\mathcal{V} = \{1, \dots, N\}$ denotes the set of N distributed agents and $\mathcal{E} = \{\varepsilon_{ij}\}_{i,j \in \mathcal{V}}$ represents the set of communication links

between any two adjacent agents. Let \mathcal{N}_i denote the set of all neighboring agents connected with agent i and we denote the number of agents in \mathcal{N}_i by $d_i = |\mathcal{N}_i|$. The adjacency matrix of \mathcal{G} is denoted by \mathbf{A} , where $\mathbf{A}(i, j) = 1$ if $\varepsilon_{ij} \in \mathcal{E}$ and $\mathbf{A}(i, j) = 0$ otherwise.

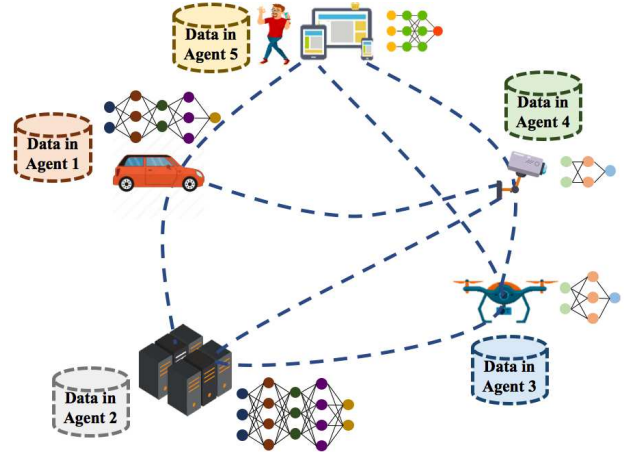


Fig. 1: The decentralized communication network of agents with heterogeneous data and system capabilities.

As shown in Fig. 1, the agents in the network are located in different positions within a global environment, leading to each agent having only a partial view of the global information. Thus, each agent $i \in \mathcal{V}$ has access to its own local training dataset $\mathcal{D}_i = \{\mathbf{x}_s, \mathbf{y}_s\}_{s=1}^{n_i}$, with data drawn from a personal data distribution over a common feature space \mathcal{X} and label space \mathcal{Y} . In the considered model, the agents in \mathcal{G} have different data distributions, known as statistical heterogeneity. Additionally, agents may possess varying system capabilities, including differences in computational power or communication capabilities, resulting in system heterogeneity among agents. We define the model retention ratio as the proportion of model that needs to be retained after pruning, denoted by $0 < r_i \leq 1$ for agent i . Then the model sparsity requirement in agent i is represented by $1 - r_i$. The model retention ratio indicates the system capacity of each agent, where a higher r_i value corresponds to greater communication or computational capacity.

Let f_i denote the local loss function of agent i and the global loss function is:

$$\min F(\mathbf{V}) := \frac{1}{N} \sum_{i=1}^N f_i(\mathbf{v}_i), \quad (1)$$

where \mathbf{v}_i denotes the model parameters of node i , and $\mathbf{V} = [\mathbf{v}_1, \mathbf{v}_2, \dots, \mathbf{v}_N]$ represents the collection of model parameters across all nodes. In supervised learning, $f_i(\mathbf{v}_i)$ stands for the expected loss over the local data distribution of agent i , defined by

$$f_i(\mathbf{v}_i) := \mathbb{E}_{\mathcal{D}_i} [l_i(\mathbf{v}_i; \mathbf{x}_s, \mathbf{y}_s)], \quad (2)$$

where $l_i(\mathbf{v}_i; \mathbf{x}_s, \mathbf{y}_s)$ measures the prediction error for label \mathbf{y}_s given the input \mathbf{x}_s and the model parameters $\mathbf{v}_i, \forall i \in \mathcal{V}$. We decouple the local model parameters \mathbf{v}_i into the Hadamard product of real-valued parameters \mathbf{w}_i and binary masks \mathbf{m}_i , i.e., $\mathbf{v}_i = \mathbf{w}_i \odot \mathbf{m}_i, \forall i \in \mathcal{V}$. The binary mask \mathbf{m}_i has the

same shape as the model parameters, with each entry being 0 or 1. Due to the statistical and system heterogeneity among agents, this personalized learning task's, optimization problem (1) does not include consensus constraints on the model parameters. Moreover, f_i is assumed to be L -smooth. In this work, we consider the synchronous settings, where each agent aggregates the information until it receives all the messages from neighboring nodes. This may require more training time, due to the heterogeneous communication or learning delays. However, such synchronous settings can improve the stability of the algorithm.

Before developing our algorithm, we introduce the lottery ticket hypothesis and the model learning procedure based on binary masks.

B. Lottery Ticket and Binary Mask Update

The lottery ticket hypothesis (LTH) was proposed and experimentally verified in [38] stating that any randomly initialized network contains lottery tickets. Here the lottery tickets are sparse subnetworks that can be trained to achieve the performance of the fully-trained original network, as shown in Fig. 2(b). More recently, the work [39] proposed a stronger version of the hypothesis, depicted in Fig. 2(c): a network with random weights contains sub-networks that can approximate any given sufficiently-smaller neural networks with high probability, even without training. This concept, termed the Strong Lottery Ticket Hypothesis (SLTH) in [40], has been rigorously proven for dense networks [37] and convolutional neural networks [41].

However, it is always computationally challenging to find any winning lottery tickets with competitive performance on the given data. The work [36] demonstrated the combination of pruning mask and weights can create an efficient subnetwork found within the larger network, while the work [33] proposed an effective way that involves updating binary masking tensor while keeping real-valued parameters fixed.

Specifically, since the binary tensor \mathbf{m}_i is discrete and cannot be directly updated using gradient descent, we introduce a real-valued mask tensor \mathbf{z}_i with the same size as \mathbf{m}_i . By updating \mathbf{z}_i and ranking the absolute values of its entries, each binary entry in \mathbf{m}_i can be determined as $\mathbf{m}_i(t) = \text{Thres}(\text{abs}(\mathbf{z}_i(t)))$, where $\text{Thres}(\cdot)$ is an entry-wise threshold operation defined as:

$$\text{Thres}(a) = \begin{cases} 0 & a \leq T_a, \\ 1 & a > T_a. \end{cases} \quad (3)$$

Here T_a is chosen according to the required model retention ratio. Considering the different scale among layers in deep neural network, the threshold operation is conducted in a layer-wise way. For the real-valued mask tensor in layer l , denoted as $\mathbf{z}_{i,l}$, we rank all entries from largest to smallest, and select the $100 \times r_i$ -th entry as T_a . In this way, the entries of 1 in the binary mask tensor $\mathbf{m}_{i,l}$ correspond to the r_i largest amplitudes in $\mathbf{z}_{i,l}$. Due to the system heterogeneity, the value of r_i may differ among agents, leading to different sparsity of the binary mask tensors.

In the k -th iteration, according to the back propagation, we can get the approximated update rule of \mathbf{z}_i based on gradient descent:

$$\begin{aligned} \mathbf{z}_i^{(k)} &= \mathbf{z}_i^{(k-1)} - \eta \frac{\nabla f_i}{\nabla \mathbf{v}_i} \times \frac{\nabla \mathbf{v}_i}{\nabla \mathbf{m}_i} \times \frac{\nabla \mathbf{m}_i}{\nabla \mathbf{z}_i} \\ &\approx \mathbf{z}_i^{(k-1)} - \eta \frac{\nabla f_i}{\nabla \mathbf{v}_i} \times \frac{\nabla \mathbf{v}_i}{\nabla \mathbf{m}_i} \times \text{sign}(\mathbf{z}_i^{(k-1)}), \end{aligned} \quad (4)$$

where the gradient $\nabla \mathbf{m}_i / \nabla \mathbf{z}_i$ cannot be explicitly calculated, so we approximate it using $\text{sign}(\mathbf{z}_i^{(k-1)})$, a method also applied in the training of binary neural networks. In each iteration, parameters of the real-valued mask tensor \mathbf{z}_i are updated according to (4). Subsequently, the binary mask tensor \mathbf{m}_i is obtained through the threshold operation defined in (3).

III. ALGORITHM DEVELOPMENT

In this section, we firstly propose the distributed strong lottery ticket hypothesis (DSLTH), which serves as the theoretical foundation for the proposed method. The proposed DSLTH justifies the designed framework where only binary masks are transmitted and updated among agents. Next, we introduce a regularization term with group sparsity and design the procedure for obtaining the binary mask tensor. Finally, the limited information embedded in these binary mask tensors makes it challenging to effectively fuse the mask tensors from neighboring, particularly in scenarios with node heterogeneity. To resolve this issue, we develop a distributed training algorithm tailored for the considered scenario and give the Mask-based Communication-Efficient Personalized Learning Algorithm (MCE-PL).

A. Distributed Lottery Ticket Hypothesis

According to the strong lottery ticket hypothesis, there exist subnetworks within a large neural network that can achieve roughly the comparable accuracy as the target network. At the same time, recent studies in FL [12, 13, 33] have demonstrated that, under the non-i.i.d. condition and the diverse system capabilities of agents, different extraction of subnetworks from a large, well-trained model can achieve high personalized accuracy. Building on these observations, we propose a DSLTH for distributed learning systems as follows and shown in Fig. 2(d).

Distributed strong lottery ticket hypothesis: *In distributed learning scenarios characterized by both data and node heterogeneity, there exist heterogeneous subnetworks among agents that can be extracted from a global and randomly initialized large (over-parameterized) neural network, performing well on local data distribution with high probability.*

Note that the rigorous proof of DSLTH in general conditions is as challenging as proving LTH and SLTH [37, 40, 41]. Therefore, in this work, we present a theoretical proof of DSLTH under constrained CNN conditions in Section IV. Additionally, we empirically verify the hypothesis in more general settings through testing simulations, as described in Section V-A. We leave a more comprehensive evaluation, both experimental and theoretical, to future works.

Based on the proposed DSLTH, the real-valued parameters \mathbf{w}_i are initialized and fixed the same among agents $i \in \mathcal{V}$,

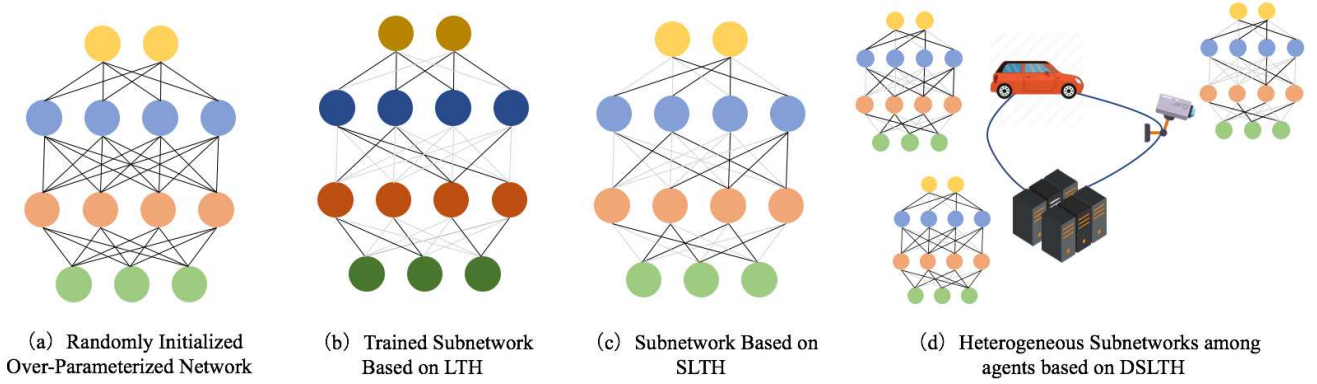


Fig. 2: Illustration of the lottery ticket hypothesis, strong lottery ticket hypothesis and distributed strong lottery ticket hypothesis: In (a), (c) and (d), the weight parameters are of initialized values, while the circles of darker color in (b) indicate trained weight parameters.

denoted by w for simplicity. The initialized real-valued parameters make up the over-parameterized neural network, while the agents aim to find their own subnetworks that is tailored to its specific statistical distribution and system requirements. To achieve this, each agent prunes its local personalized model by updating and sharing the binary mask tensor m_i . Compared with other methods based on LTH, such as those in [15, 24] and as illustrated in Fig. 2(b), the key difference is whether real-valued parameters are transmitted or updated, which significantly reduces the communication cost in our approach.

B. Regularization and Binary Tensor

Updating z_i directly according to (4) may result in binary mask tensor with non-structured sparsity, and this irregular memory access can adversely impact practical acceleration in hardware implementations, leading to higher costs compared to structured sparsity. To resolve this issue, we incorporate a structured sparsity regularization term into the loss functions of the agents.

Specifically, for the l -th convolutional layer, the real-valued mask tensor is denoted by $z_{i,l} \in \mathbb{R}^{O_l \times I_l \times H_l \times W_l}$, where O_l, I_l, H_l, W_l represent the dimensions of output filter, input channel, kernel height and kernel width. Group Lasso can effectively zero out all weights in certain groups, forming the basis of structured sparsity regularization. In this work, we consider the sparsity along the output filter and take the entries in one output filter as a group. Then the regularization term for the l -th convolutional layer in agent i can be expressed as follows:

$$R(z_{i,l}) = \lambda \left(\sum_{o_l=1}^{O_l} \|z_{i,l}(o_l, :, :, :)\|_2 \right), \quad (5)$$

where λ is the regularization parameter used to balance the loss and the pruning criterion. Note that there may exist different forms of regularizers with different properties [42, 43], including ℓ_1 norm, ℓ_2 norm and composite ℓ_1/ℓ_2 . In this work, we do not focus on the specific regularizers. To simplify the computation of gradients, we use the ℓ_2 norm regularization.

Similarly, for the l -th linear layer, the regularization term for the real-valued mask tensor $z_{i,l} \in \mathbb{R}^{O_l \times I_l}$ is as follows:

$$R(z_{i,l}) = \lambda \left(\sum_{o_l=1}^{O_l} \|z_{i,l}(o_l, :)\|_2 \right). \quad (6)$$

By summing up (5) and (6) across all layers, we obtain the final regularization term as follows:

$$R(z_i) = \lambda \sum_{l=1}^{L_c} \left(\sum_{o_l=1}^{O_l} \|z_{i,l}(o_l, :, :, :)\|_2 \right) + \lambda \sum_{l=1}^{L_l} \left(\sum_{o_l=1}^{O_l} \|z_{i,l}(o_l, :)\|_2 \right), \quad (7)$$

where L_c and L_l represent the number of convolutional and linear layers, respectively. Then, the global loss function, with fixed global real-valued parameters w and updatable real-valued mask tensors z_i can be expressed as follows:

$$\min F(\mathbf{Z}) := \frac{1}{N} \sum_{i=1}^N f_i(w, z_i), \quad (8)$$

where \mathbf{Z} is the set of z_i for all node $i \in \mathcal{N}$. Here the local loss function of node i is as follows:

$$f_i(w, z_i) := \mathbb{E}_{\mathcal{D}_i} [l_i(w, z_i; \mathbf{x}_s, \mathbf{y}_s)] + R(z_i). \quad (9)$$

As discussed in Section II-B, to obtain the binary mask tensor from the real-valued mask tensor, we use the threshold method (3). It is important to note that we still use the entry-wise ranking in each layer, instead of ranking the sum of absolute values in one filter and zeroing out those filters with smaller value. Although the latter method can ensure filter-wise sparsity after each iteration, it suffers from poor robustness and convergence properties. Therefore, we apply entry-wise ranking, along with the group sparsity regularization term, which regularizing the parameter tensor in each layer to the become structurally sparse. In this process, the hardware cost is reduced while guaranteeing the convergence performance.

Meanwhile, through experiments, we observe that the entry-wise ranking, combined with the structural sparsity regularization, may lead to a small number of non-zero entries in some filters. In such condition, these entries may have limited impact on the neural network accuracy while significantly increasing

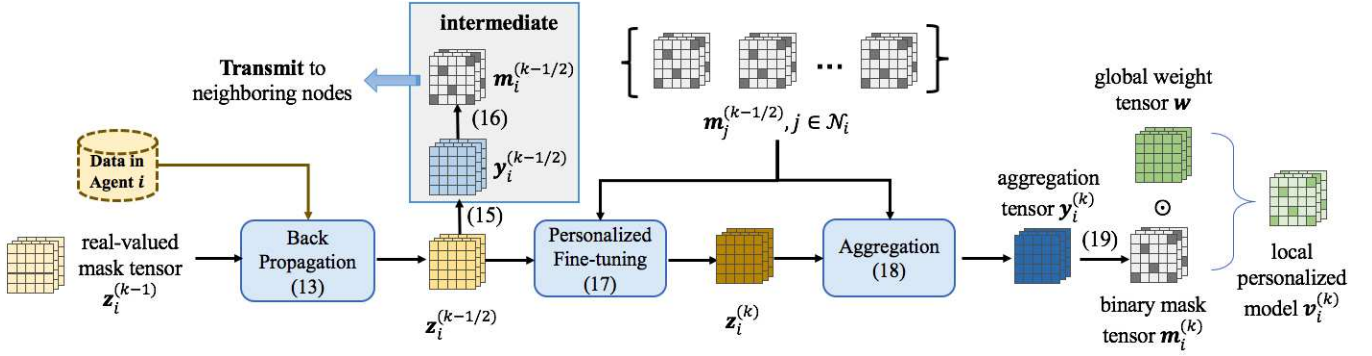


Fig. 3: The algorithm flowchart of the proposed MCE-PL in the k -th iteration for node i : The updated and fused binary mask tensor $\mathbf{m}_i^{(k)}$ is obtained based on the aggregation tensor $\mathbf{y}_i^{(k)}$. $\mathbf{y}_i^{(k)}$ combines the information from $\mathbf{z}_i^{(k)}$ and the binary information $\mathbf{m}_j^{(k-1/2)}$ received from neighboring nodes $j \in \mathcal{N}_i$, where $\mathbf{z}_i^{(k)}$ is updated through back propagation and personalized fine-tuning.

the hardware cost. To resolve this issue, we introduce an additional rule, denoted as $\text{Fil}[\cdot]$, which acts as follows: when the number of non-zero entries in one filter is below a threshold, all entries in the corresponding filter of the binary mask tensor are set to 0. This operation can further enhance the structural sparsity of the local model. Then, for node i , the binary mask tensor in layer l can be obtained from the real-valued tensor as follows:

$$\mathbf{m}_{i,l} = \text{Fil}[\text{Thres}(\mathbf{z}_{i,l})]. \quad (10)$$

C. Aggregation Algorithm Design

The analysis in [36] shows the effectiveness of model learning using binary mask tensor. Experiments verify the hypothesis that the masking operation tends to direct toward the values they would have reached during training. Based on this observation, the entries in the mask tensor indicate whether the corresponding real-valued parameters are expected to approach 0. In distributed learning scenarios, although the data distribution among agents are non-i.i.d., the agents are located in some global environment and their personalized data distributions represent partial views of the global data distribution. Thus, certain correlations exist among agents, which can be leveraged through collaboration to enhance each model's performance. Since binary mask tensors contain specific information about the model parameters, they can be aggregated among agents to improve local model performance through appropriate algorithm design.

The method in [33] performs aggregation by taking intersection between the local updated mask and the other masks, and then initializing the real-valued mask tensor according to this result. However, this procedure is not suitable for heterogeneous system scenarios, where the retained model in each agent tends to converge to the smallest one, and the computational capacity in each agent cannot be sufficiently used. Thus, we need to carefully design the mask aggregation algorithm that allows the fusion of information from neighboring nodes while preserving the heterogeneity of devices. Given that the binary mask tensors received by each agent carry very limited information, it is challenging to exploit model relativity or to derive explicit aggregation weights as done in [3]. Therefore, we propose an alternative

update framework based on a simple but effective method in personalized learning, which combines aggregation through averaging with an additional step of personalized fine-tuning.

We first discuss the aggregation procedure. Based on the observation from experiments, we find the key issue of the aggregation method: The direct aggregation of binary mask tensors on \mathbf{z}_i consistently results in low accuracy and poor stability of the algorithm. This occurs because the direct operation on \mathbf{z}_i cause the local model to be heavily influenced by the neighboring binary mask tensors, whose limited information especially under non-i.i.d. condition leads to severe deviation of local model. To address this problem, in addition to the real-valued mask tensor \mathbf{z}_i , we introduce an another intermediate tensor \mathbf{y}_i in each node, named as aggregation tensor. The aggregated binary mask in each agent is obtained based on this aggregation tensor.

However, it is still challenging to fuse the binary information from $\mathbf{m}_j, j \in \mathcal{N}_i$ into the real-valued aggregation tensor. As discussed above, in the binary mask tensor, the indices of those 1 entries indicate larger amplitude of entries in the real-valued tensor. Based on this observation, a certain amplitude is expected to be added to the corresponding indices of the aggregated tensor. However, due to the limited information in the binary tensors, the explicit amplitude to be added could not be accurately computed. To address this challenge, we design an adaptive aggregation model to obtain the aggregation tensor \mathbf{y}_i based on local \mathbf{z}_i and the received binary mask tensors from neighboring nodes.

Considering the amplitude of \mathbf{z}_i may vary among different agents, different layers in one agent and even across different iteration steps, we design an adaptively-defined value $\text{mean}[\text{abs}(\tilde{z}_{i,l})]$ to approximate the amplitude to be added for the l -th layer in node i . Here the operation $\text{abs}(\cdot)$ means taking absolute values of all entries in the tensor and $\text{mean}[\cdot]$ take average of all entries in the tensor to get the mean value. The notation \tilde{z} indicates that the tensor is used for external model operation and can be treated as a constant, which will not be involved in the gradient descent process. The aggregation is then performed by taking average of the received binary tensor. By considering the sign of \mathbf{z}_i , we derive the aggregation model of layer l for agent i as follows:

$$\mathbf{y}_{i,l} = \mathbf{z}_{i,l} + \left\{ \text{mean}[\text{abs}(\tilde{z}_{i,l})] \times \text{sign}(\tilde{z}_{i,l}) \right\}$$

$$\odot \left(\frac{1}{|\mathcal{N}_i|} \sum_{j \in \mathcal{N}_i} \mathbf{m}_{j,l} \right). \quad (11)$$

Based on the aggregation tensor, the corresponding aggregated binary mask tensor can be obtained through

$$\mathbf{m}_{i,l} = \text{Fil}[\text{Thres}(\mathbf{y}_{i,l})]. \quad (12)$$

On the other hand, the fine-tuning step with local data can adjust the direction of parameter updates to better align with the local data distribution. Inspired by this, we introduce a personalized fine-tuning step in each iteration to prevent model deviation caused by the limited information in mask tensors and the heterogeneous data distribution among agents.

The designed procedure is thus composed of three steps in each iteration: back propagation, personalized fine-tuning and model aggregation as shown in Fig. 3. In the following we describe the three steps one by one.

Back Propagation. Given the fixed real-valued parameters \mathbf{w} , together with the binary mask tensor updated in the last iteration $\mathbf{m}_i^{(k-1)}$, the forward computation can be conducted as follows:

$$f_i(\mathbf{v}_i^{(k-1)}) = f_i(\mathbf{w} \odot \mathbf{m}_i^{(k-1)}). \quad (13)$$

Based on the loss computed through the forward process, the gradient descent of \mathbf{z}_i can be derived as follows:

$$\begin{aligned} \mathbf{z}_i^{(k-1/2)} &= \mathbf{z}_i^{(k-1)} - \eta \frac{\nabla f_i}{\nabla \mathbf{v}_i} \times \frac{\nabla \mathbf{v}_i}{\nabla \mathbf{m}_i} \times \frac{\nabla \mathbf{m}_i}{\nabla \mathbf{z}_i} \\ &\approx \mathbf{z}_i^{(k-1)} - \eta \frac{\nabla f_i}{\nabla \mathbf{v}_i} \times \frac{\nabla \mathbf{v}_i}{\nabla \mathbf{m}_i} \times \text{sign}(\mathbf{z}_i^{(k-1)}), \end{aligned} \quad (14)$$

where the gradient of \mathbf{z}_i is given below,

$$G(\mathbf{z}_i^{(k-1)}) = \frac{\nabla f_i}{\nabla \mathbf{v}_i} \times \frac{\nabla \mathbf{v}_i}{\nabla \mathbf{m}_i} \times \text{sign}(\mathbf{z}_i^{(k-1)}). \quad (15)$$

According to (11), the gradient of \mathbf{z}_i equals to \mathbf{y}_i , where the second term can be treated as an adaptive constant. Then, based on $\mathbf{z}_i^{(k-1/2)}$, the intermediate aggregation tensor \mathbf{y}_i and the intermediate binary tensor \mathbf{m}_i can be obtained as follows:

$$\mathbf{y}_{i,l}^{(k-1/2)} = \mathbf{z}_{i,l}^{(k-1/2)} + \left\{ \text{mean} \left[\text{abs}(\tilde{\mathbf{z}}_{i,l}^{(k-1/2)}) \right] \right. \quad (16a)$$

$$\left. \times \text{sign}(\tilde{\mathbf{z}}_{i,l}^{(k-1/2)}) \odot \left(\frac{1}{|\mathcal{N}_i|} \sum_{j \in \mathcal{N}_i} \mathbf{m}_{j,l}^{(k-3/2)} \right) \right\},$$

$$\mathbf{m}_{i,l}^{(k-1/2)} = \text{Fil}[\text{Thres}(\mathbf{y}_{i,l}^{(k-1/2)})]. \quad (16b)$$

where the binary mask tensors from neighboring nodes $\mathbf{m}_{j,l}^{(k-3/2)}$ are those received in the former iteration. Then each agent shares its intermediate binary mask tensor $\mathbf{m}_i^{(k-1/2)}$ to its neighboring nodes.

Personalized Fine-tuning. As mentioned before, to update the model in each agent towards the personalized data distribution, we add the fine-tuning step in each iteration. This step is essential especially in the mask-based aggregation, where the limited yet biased information from the binary tensors may lead to severe performance degradation. Specifically, considering the sparsity of those binary mask tensors, the aggregation makes an impact on some limited entries. Thus, based on the received binary tensors $\mathbf{m}_j^{(k-1/2)}$, the fine-tuning is conducted on those entries which will be affected by the

Algorithm 1: MCE-PL

```

1 for node  $i = 1, 2, \dots, N$  do
2   Initialize the real-valued parameters  $\mathbf{w}$  and binary
   mask tensor from neighboring nodes
    $\mathbf{m}_j^{(0)}, j \in \mathcal{N}_i$ . Set  $k = 0$ .
3 while not converge do
4    $k = k + 1$ 
5   for node  $i = 1, 2, \dots, N$  do
6     Randomly select a batch of data from local
     training data set  $\{\mathbf{x}_s, \mathbf{y}_s\} \in \mathcal{D}_i$ .
7     Compute the loss by (9).
8     Update  $\mathbf{z}_i^{(k-1/2)}$  by back propagation and get
      $G(\mathbf{z}_i^{(k-1)})$ .
9     Obtain  $\mathbf{y}_i^{(k-1/2)}$  and  $\mathbf{m}_i^{(k-1/2)}$  by (16a) and
     (16b).
10    Transmit  $\mathbf{m}_i^{(k-1/2)}$  to all neighboring nodes.
11  for node  $i = 1, 2, \dots, N$  do
12    Personalized fine-tune and get the updated
     $\mathbf{z}_i^{(k)}$  by (17).
13    Aggregate the information and get the
    aggregated binary tensor  $\mathbf{m}_i^{(k)}$  by (19).
14 Output the personalized model in each agent.

```

mask aggregation. Moreover, the approximated gradient of \mathbf{z}_i obtained and stored before is utilized here to reduce the computational cost. Then we can get the personalized fine-tuning step as follows:

$$\mathbf{z}_i^{(k)} = \mathbf{z}_i^{(k-1/2)} - \eta \times G(\mathbf{z}_i^{(k-1)}) \odot \left(\frac{1}{|\mathcal{N}_i|} \sum_{j \in \mathcal{N}_i} \mathbf{m}_j^{(k-1/2)} \right). \quad (17)$$

This fine-tuning step allows the model to aggregate in the subsequent step based on personalized needs, thereby enabling effective information fusion.

Aggregation. Based on the fine-tuned $\mathbf{z}_i^{(k)}$, the aggregation of binary mask tensors in the aggregation tensor can be expressed by,

$$\begin{aligned} \mathbf{y}_{i,l}^{(k)} &= \mathbf{z}_{i,l}^{(k)} + \left\{ \text{mean} \left[\text{abs}(\tilde{\mathbf{z}}_{i,l}^{(k)}) \right] \times \text{sign}(\tilde{\mathbf{z}}_{i,l}^{(k)}) \right. \\ &\quad \left. \odot \left(\frac{1}{|\mathcal{N}_i|} \sum_{j \in \mathcal{N}_i} \mathbf{m}_{j,l}^{(k-1/2)} \right) \right\}. \end{aligned} \quad (18)$$

Then, the aggregated binary tensor can be obtained as follows:

$$\mathbf{m}_{i,l}^{(k)} = \text{Fil}[\text{Thres}(\mathbf{y}_{i,l}^{(k)})]. \quad (19)$$

Note that, the aggregation step (19) is conducted after the personalized fine-tuning, which is different from the typical aggregation-and-fine-tuning procedure. This is necessary because the introduced aggregation tensor needs to be derived based on the fine-tuned \mathbf{z}_i . According to the above three steps, the Mask-based Communication-Efficient Personalized Learning Algorithm (MCE-PL) can be summarized in Algorithm 1.

Note that, each agent does not need to keep the intermediate tensors $\mathbf{y}_i^{(k-1/2)}$ and $\mathbf{y}_i^{(k)}$ after obtaining $\mathbf{m}_i^{(k-1/2)}$ and $\mathbf{m}_i^{(k)}$. Likewise, $\mathbf{m}_i^{(k-1/2)}$ can be relaxed after computing $\mathbf{z}_i^{(k-1/2)}$.

Remark 1. Computational Complexity. *The computational complexity has been widely investigated in the context of real-value-based updating, with the derived convergence rate. For distributed stochastic gradient descent (DSGD) [4], its convergence rate is $\mathcal{O}(\frac{1}{\sqrt{NT}})$, and the computational complexity can be derived as $\mathcal{O}(\frac{1}{\epsilon^2})$ concerning the ϵ -approximation solution. However, the convergence analysis for the binary-mask-based updating is still a challenging topic, even in centralized settings [38]. So here we simplify the computational complexity analysis in one iteration. In each iteration, the (intermediate) aggregation tensor \mathbf{y}_i and the (intermediate) binary tensor \mathbf{m}_i are updated in a layer-wise way within each agent. If we further take the aggregation in (16a) and (18) into consideration, under large N , the total number of neighboring nodes can be approximated by $\mathcal{O}(N^2p)$ with connectivity probability p . Thus, given N agents, the computational complexity over the network in one iteration is $\mathcal{O}(N^2Lp)$ considering the neural network with L layers. Compared with FedProx [7], the computation cost w.r.t. time and energy of the proposed algorithm may increase with the additional pruning steps defined by (16b) and (19). Compared with LotteryFL [15], the computation cost of MCE-PL is lightly higher with the personalized fine-tuning step.*

Remark 2. Privacy and Security Analysis. *Note that our approach leverages a unique parameterization in which each local model is obtained by the Hadamard product of fixed global parameters and personalized binary masks. This configuration not only introduces structural obfuscation—effectively discretizing the parameter space and introducing quantization noise into the local model—but also achieves information fragmentation by restricting updates solely to the binary masks while keeping the global parameters constant. Consequently, the temporal correlation between successive updates is disrupted, significantly mitigating the risks of model inversion and information leakage common in conventional gradient-based methods.*

IV. THEORETICAL PROOF OF DSLTH

In this section, we give the theoretical proof of the proposed distributed strong lottery ticket hypothesis under the statistical heterogeneous conditions, based on the rigorous proof of SLTH in [41]. For the sake of simplicity, we consider the convolutional neural network in a restricted setting, which is defined as $f : [0, 1]^{D \times D \times O_0} \rightarrow \mathbb{R}^{D \times D \times O_L}$ with the form

$$f(\mathbf{x}) = \mathbf{v}_L * \sigma(\mathbf{v}_{L-1} * \cdots * \sigma(\mathbf{v}_1 * \mathbf{x})). \quad (20)$$

Here, $*$ denotes the convolution operation, $\sigma(\cdot)$ represents the ReLU activation function and $\mathbf{v}_l \in \mathbb{R}^{O_l \times O_{l-1} \times d_l \times d_l}$ represents the convolution weight in the l -th layer, where the convolutions have no bias and are suitably padded with zeros. Note f does not include additional operations such as stride or average pooling, a more general analysis is deferred to future works.

In the distributed scenarios with heterogeneous data, we consider an arbitrary pair of nodes, whose relationship can be extended to those nodes in the whole decentralized network without loss of generality. Use the subscript 1 and 2 to denote the arbitrary two nodes, and their local datasets are denoted by $\mathcal{D}_1 = \{\mathbf{x}_{1,s}, \mathbf{y}_{1,s}\}$ and $\mathcal{D}_2 = \{\mathbf{x}_{2,s}, \mathbf{y}_{2,s}\}$, including both training and testing data due to the personalized problem. The two local datasets have personal distribution over some common feature space \mathcal{X} and label space \mathcal{Y} , with the dimension $D \times D \times I_0$ of $\mathbf{x}, \forall \mathbf{x} \in \mathcal{X}$. We define the two local models as f_1 and f_2 for any two nodes, which are sufficiently and independently trained by local dataset from the same initialization f_0 with the architecture/form in (20).

For a tensor \mathbf{a} , the notation $\|\mathbf{a}\|_1$ is its ℓ_1 norm defined as the sum of the absolute values of each entry in \mathbf{a} . $\|\mathbf{a}\|$ is the ℓ_2 norm, where $\|\mathbf{a}\|^2$ equals to the sum of the each entry's square value. And the notation $\|\mathbf{a}\|_{\max}$ refers to its maximum norm as the maximum among the absolute value of each entry. Define a class of functions from $[0, 1]^{D \times D \times O_0}$ to $\mathbb{R}^{D \times D \times O_L}$ as \mathcal{F} such that for each $f \in \mathcal{F}$, $f(\mathbf{x}) = \mathbf{v}_L * \sigma(\mathbf{v}_{L-1} * \cdots * \sigma(\mathbf{v}_1 * \mathbf{x}))$, where for each $l \in [L]$, the weight tensor $\mathbf{v}_l \in [-1, 1]^{O_l \times O_{l-1} \times d_l \times d_l}$ and $\|\mathbf{v}_l\|_1 \leq 1$.

We firstly make some assumptions for simplicity of analysis.

Assumption 1. *In the dataset, each entry of the features is in the range of $[0, 1]$, i.e., $\mathbf{x} \in [0, 1]^{D \times D \times I_0}, \forall \mathbf{x} \in \mathcal{X}$.*

Assumption 2. *The two sufficiently and independently trained networks $f_1, f_2 \in \mathcal{F}$.*

Assumption 3. *The output distance of f_1 and f_2 can be upper bounded by $\sup_{\mathbf{x} \in \mathcal{X}} \|f_1(\mathbf{x}) - f_2(\mathbf{x})\|_{\max} \leq \alpha_u$, with the different parameters indicated by $\inf_{\mathbf{x} \in \mathcal{X}} \|f_1(\mathbf{x}) - f_2(\mathbf{x})\|_{\max} \geq \alpha_l$.*

Among these assumptions, Assumption 1 can be satisfied through data normalization. Assumption 2 can be satisfied through the proper initialization and training process such that there exist f_1 and f_2 in the class of \mathcal{F} . The upper bound in Assumption 3 measures the distance between the output of two models given the same input. It is proposed and rational considering the same initialization f_0 and the correlation between the local datasets in the two nodes, which are located in a global data distribution. It should be noted that the value α_u would be related to the distance between the parameters of f_1 and f_2 , which can be further correlated to distance between gradients in the training process. We defer to future works for a more comprehensive investigation in such non i.i.d. conditions. On the other hand, considering the personalized data distribution, the difference of the learned models can be indicated by $\inf_{\mathbf{x} \in \mathcal{X}} \|f_1(\mathbf{x}) - f_2(\mathbf{x})\|_{\max} \geq \alpha_l$, meaning that for any data sample, there exists certain distance between the output, which is rational due to the independent training in the non-i.i.d. condition. Then the theory on SLTH in centralized condition is shown as follows:

Lemma 1. *(Theorem 1 in [41] for SLTH) Consider a convolutional network with L layers. ϵ and C are two positive constant. Let $O_l, I_l \in \mathbb{N}$ with $I_l \geq CO_l \log \frac{O_{l-1} O_l d_l^2 L}{\min\{\epsilon, \delta\}}$. Define $\mathbf{w}_{2l-1} \in \mathbb{R}^{I_l \times O_{l-1} \times d_l \times d_l}$, $\mathbf{w}_{2l} \in \mathbb{R}^{O_l \times I_l \times 1 \times 1}$. Define the corresponding binary mask tensors with the same shape, i.e.,*

$\mathbf{m}_{2l-1} \in \{0, 1\}^{\text{size}(\mathbf{w}_{2l-1})}$ and $\mathbf{m}_{2l} \in \{0, 1\}^{\text{size}(\mathbf{w}_{2l})}$. The entries of $\mathbf{w}_1, \dots, \mathbf{w}_{2L}$ are i.i.d. random variables from the uniform distribution in $[-1, 1]$. Define the random 2L-layer CNN $g : [0, 1]^{D \times D \times O_0} \rightarrow \mathcal{R}^{D \times D \times O_l}$ as:

$$g(\mathbf{x}) = \mathbf{w}_{2L} * \sigma(\dots \sigma(\mathbf{w}_1 * \mathbf{x})). \quad (21)$$

Its pruned version is defined as:

$$g_{\mathbf{m}}(\mathbf{x}) = (\mathbf{w}_{2L} \odot \mathbf{m}_{2L}) * \sigma[\dots \sigma[(\mathbf{w}_1 \odot \mathbf{m}_1) * \mathbf{x}].$$

Then we can choose constant C independently from other parameters so that with probability at least $1 - \delta$, the following holds for every $f \in \mathcal{F}$:

$$\inf_{\mathbf{m} \in \{0, 1\}^{\text{size}(\mathbf{w})}} \sup_{\mathbf{x} \in [0, 1]^{D \times D \times O_0}} \|f(\mathbf{x}) - g_{\mathbf{m}}(\mathbf{x})\|_{\max} \leq \varepsilon. \quad (22)$$

In (22) of Lemma 1, \inf indicates the existence of such pruned network. Then based on Lemma 1 and the definitions in it, in the distributed condition, we can give the following major theorem for an arbitrary pair of nodes denoted by subscript 1 and 2 as talked above:

Theorem 1. (DSLTH) Suppose the trained model $f_1, f_2 \in \mathcal{F}$. Define the random 2L-layer CNN g as that in (21). Its pruned versions in node 1 and node 2 are respectively defined as:

$$g_{\mathbf{m}_1}(\mathbf{x}) = (\mathbf{w}_{2L} \odot \mathbf{m}_{1,2L}) * \sigma[\dots \sigma[(\mathbf{w}_1 \odot \mathbf{m}_{1,1}) * \mathbf{x}],$$

$$g_{\mathbf{m}_2}(\mathbf{x}) = (\mathbf{w}_{2L} \odot \mathbf{m}_{2,2L}) * \sigma[\dots \sigma[(\mathbf{w}_1 \odot \mathbf{m}_{2,1}) * \mathbf{x}].$$

Then there exist binary mask tensors \mathbf{m}_1 and \mathbf{m}_2 , such that the pruned networks in node 1 and 2 have the following property with probability at least $(1 - \delta)^2$:

$$\sup_{\mathbf{x} \in \mathcal{X}} \|f_1(\mathbf{x}) - g_{\mathbf{m}_1}(\mathbf{x})\|_{\max} \leq \varepsilon_1, \quad (23)$$

$$\sup_{\mathbf{x} \in \mathcal{X}} \|f_2(\mathbf{x}) - g_{\mathbf{m}_2}(\mathbf{x})\|_{\max} \leq \varepsilon_2. \quad (24)$$

Moreover, the pruned networks between node 1 and 2 has the following correlation with probability $(1 - \delta)^2$:

$$\sup_{\mathbf{x} \in \mathcal{X}} \|g_{\mathbf{m}_1}(\mathbf{x}) - g_{\mathbf{m}_2}(\mathbf{x})\|_{\max} \leq \varepsilon_1 + \varepsilon_2 + \alpha_u, \quad (25)$$

and the heterogeneity with probability $(1 - \delta)^2$:

$$\begin{aligned} & \inf_{\mathbf{x} \in \mathcal{X}} \|g_{\mathbf{m}_1}(\mathbf{x}) - g_{\mathbf{m}_2}(\mathbf{x})\|_{\max} \\ & \geq \min\{|\varepsilon_1 + \varepsilon_2 - \alpha_l|, |\varepsilon_1 + \varepsilon_2 - \alpha_u|, |\alpha_l|\}. \end{aligned} \quad (26)$$

Proof: See Appendix A. ■

Theorem 1 establishes the theoretical foundation for DSLTH and the proposed framework. (23) and (24) demonstrate the good performance of the locally pruned subnetworks. Additionally, under the same real-valued parameters in $g_{\mathbf{m}_1}(\mathbf{x})$ and $g_{\mathbf{m}_2}(\mathbf{x})$, (25) reveals the correlation between the binary mask tensors \mathbf{m}_1 and \mathbf{m}_2 , illustrating the effectiveness of inter-agent correlation. Meanwhile, (26) indicates their heterogeneity and the necessity of personalization.

It should be noted that Theorem 1 only verifies DSLTH in heterogeneous data distribution, without showing the impact of system heterogeneity. Moreover, Theorem 1, following Lemma 1, only focuses on the convolutional layers with the specified form of g , which is not general to practical deep

neural networks that combine other type of layers. To further investigate the proposed DSLTH, we refer to simulations presented in Section V-A.

V. NUMERICAL EXPERIMENTS

In this section, we first experimentally verify the proposed distributed strong lottery ticket hypothesis, to show its effectiveness in data and node heterogeneity. Then the performance of the proposed MCE-PL is simulated and compared with other methods, to show its improved accuracy, faster convergence rate and communication-efficiency under the heterogeneous scenario. Consider the 10-class classification problem in CIFAR-10 dataset and apply the widely-used AlexNet architecture in each agent, which is made of three 5×5 convolutional layers, each followed by a 3×3 max pooling layer with stride 2, and two fully connected layers.

A. Verification of Distributed Strong Lottery Ticket Hypothesis

In addition to the analysis in Section III-A and theoretical proof in Section IV, in this subsection we verify the proposed DSLTH through simulations. Specifically, we choose three agents, each with three different labels in CIFAR-10 dataset. Note here we mainly aim to validate the performance of the pruned subnetworks, and the analytical results in IV cannot be practically applied here. Thus, different from the construction of f and g in Section IV, in this part we simulate a more general neural network. We want to emphasize that the experimental results aim to show the learning ability and accuracy of the pruned subnetworks. Considering the complicated construction of g in Section IV, we choose the network architecture of g the same as the baseline architecture, and is not strictly required to have twice the number of layers.

Here, in order to show the fully-trained results, each agent has all of the data samples corresponding to its labels. The parameters are initialized randomly from the uniform distribution in $[-1, 1]$. Firstly, the parameters of each model are sufficiently trained with the local heterogeneous dataset, which is named as weight update. Then based on the same and fixed initialized parameters, each local model is trained with binary mask update procedure as described in Section II-B, to obtain the pruned subnetworks of the original neural network. We set $r_i = 0.1, 0.3, 0.5$ respectively to show that some well-performed subnetworks could be found even under different r_i . The accuracy is tested every 3 update steps and the results are shown in Fig. 4.

It can be observed that the pruned subnetworks on the randomly initialized network can achieve similar accuracy as the fully-trained network, both in different agents (data heterogeneity) and different r_i (system heterogeneity). The convergence curves of the update based on mask show more oscillation compared with weight update. This is because the update based on mask is inherently a discrete update, where the updated subnetworks between iterations may lead to divergent accuracy. The above results verify the proposed DSLTH in a simple yet efficient way. Based on these fundamental results, in the following we simulate on the proposed method MCE-PL and compare it with other methods.

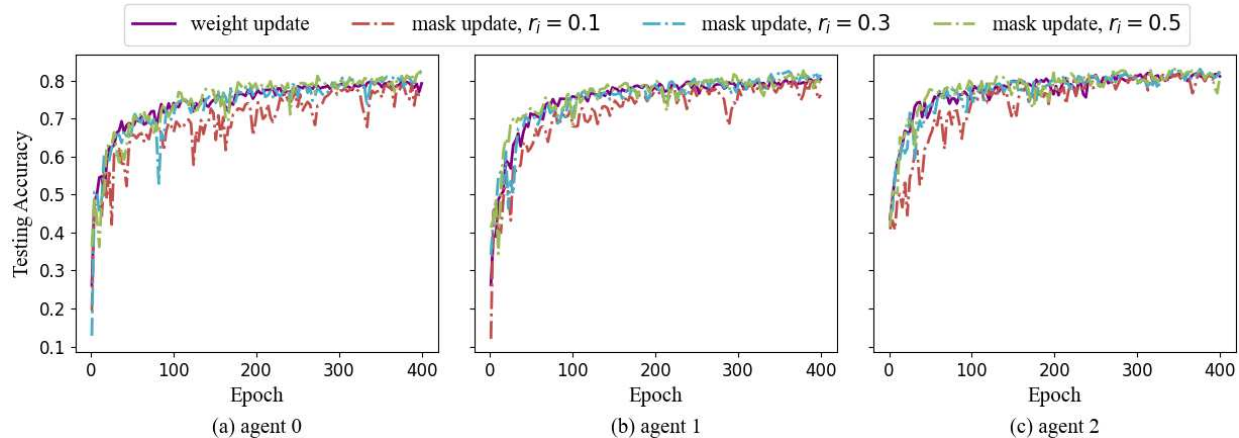


Fig. 4: The verification of the DSLTH: comparison of convergence curves between the weight-based update and the mask-based one considering $r_i = 0.1, 0.3, 0.5$ in different agents.

B. Comparison on Convergence and Communication Cost in Data Heterogeneity

In this subsection, we first compare the convergence results and communication cost of the proposed methods with other state-of-the-art algorithms considering only statistical heterogeneity. Specifically, we compare the proposed MCE-PL with the conventional decentralized stochastic gradient descent (DSGD) and FL. We also implement the FedProx [7] and LotteryFL [15] algorithms in a decentralized network, referring to them as DSGDProx and LotteryDSGD, respectively. Additionally, we compare the standalone method, where each agent performs model updates and pruning independently, as described in Section II-B, referred to as ind-mask.

We consider a multi-agent communication network with $N = 20$ nodes, whose topology is generated randomly using the *Erdos_Renyi* graph model, with the connectivity probability equal to $p = 0.5$. Consider the 10-class classification problem in CIFAR-10 dataset, where we randomly choose c_i labels assigned for each agent to reflect the non-i.i.d. data distribution. The training samples corresponding to the same label are averaged and randomly assigned to the agents, while the testing samples corresponding to local labels are all assigned to each agent for a general and comprehensive evaluation of the learned model.

We simulate the performance of algorithms under different learning rate [1.0, 0.1, 0.01, 0.001] and choose the learning rate that yields the best performance. Specifically, the learning rate is set to 1.0 for the binary mask-based algorithm MCE-PL and ind-mask and 0.1 for LotteryDSGD. For the other algorithms based on real-valued parameters, the learning rate is set to 0.01. Notably, the learning rate for z_i is much larger than that for w_i . This is due to the update mechanism for z_i , where the binary mask tensor is updated based on the sorted absolute values of its entries. Therefore, a larger learning rate induces significant changes in the amplitude of z_i , affecting the sorting results and, consequently, the binary mask tensor. The regularization term parameter is set to $\lambda = 0.001$. The results are presented in Table I, with sparsity requirements 0.3 and 0.5.

As shown in Table I, the proposed MCE-PL achieves good performance in terms of convergence accuracy. Regarding

TABLE I: The comparison of averaged testing accuracy among different algorithms under data heterogeneity.

	$c_i = 3$	$c_i = 4$	$c_i = 5$
DSGD	0.6218	0.5811	0.5660
FL	0.6112	0.6097	0.6072
DSGDProx	0.7550	0.6863	0.6143
LotteryDSGD (0.3)	0.6687	0.6212	0.5755
LotteryDSGD (0.5)	0.5612	0.6686	0.5217
ind-mask (0.3)	0.7092	0.6520	0.5876
ind-mask (0.5)	0.6934	0.6740	0.5922
MCE-PL (0.3)	0.7498	0.6951	0.6048
MCE-PL (0.5)	0.7603	0.6943	0.6244

communication cost, we compare the decentralized protocols under $c_i = 3$, focusing on LotteryDSGD with a 0.3 sparsity ratio and MCE-PL with a 0.5 sparsity ratio, which demonstrate better performance. The convergence curves, in relation to communication cost, are displayed in Fig. 5, where the proposed MCE-PL achieves the highest testing accuracy with significantly lower communication cost.

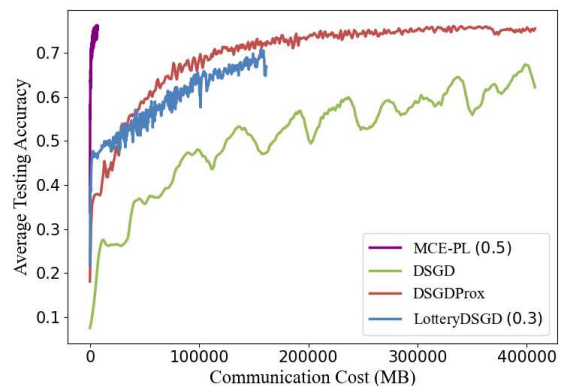


Fig. 5: The comparison of communication cost.

C. Comparison on Convergence and Communication Cost in Node Heterogeneity

All of the above baseline methods cannot be applied in node heterogeneity settings. To further show the superiority of the proposed method, we additionally consider the node

heterogeneity in this subsection. To indicate the different communication, storage and computation capabilities among agents, they have varying model retention ratios r_i . It needs to be noted that the optimization of the retention ratio among agents considering load balancing is another interesting issue, which however is not the focus of this work. So here in the simulation, we randomly generate different r_i in the range of $[0.1, 0.2, 0.3, 0.4]$ for a general test of the algorithm’s performance, and the generated sparsity requirements of agents are 0.4, 0.4, 0.3, 0.2, 0.1, 0.1, 0.1, 0.2, 0.4, 0.2, 0.4, 0.2, 0.3, 0.3, 0.4, 0.3, 0.1, 0.1, 0.3, 0.3 respectively.

We compare the proposed MCE-PL with several different algorithms in decentralized setting applying typical techniques and suited for the node heterogeneity.

- **ind-mask**: Each agent conducts model update and model pruning independently based on the method in Section II-B, without collaboration and information fusion.
- **ind-weipru**: Each agent conducts model update with conventional gradient descent on real-valued parameters. After each iteration, each agent prunes its local model according to absolute values under the requirements of model retention ratio.
- **avr-weipru**: Each agent updates its local model with conventional gradient descent on real-valued parameters, then prunes the model and transmits it to neighboring nodes. The agents then aggregate the models by taking average of the received model parameters.
- **par-weipru**: Each agent updates its local model with conventional gradient descent on real-valued parameters, then prunes the model and transmits it to neighboring nodes. The agents then aggregate the models by partially averaging.

In each iteration, the gradient is computed with stochastic gradient descent, where the batch size is 128. The learning rates are also selected from $[1.0, 0.1, 0.01, 0.001]$ and choose those with best performance. The learning rate is set to 1.0 for the binary mask-based algorithm MCE-PL and **ind-mask** and 0.001 for the other algorithms. The number of labels in each agent is set to $c_i = 4$, where the labels are assigned to each agent randomly. The convergence curves of the algorithms are shown in Fig. 6.

Fig. 6 compares the convergence performance of different algorithms. It could be observed that the oscillation exists on most of the curves, owing to the model pruning in each iteration, while the procedure **avr-weipru** reduces the divergence by taking the average. We then compare the two algorithms based on binary mask tensor, MCE-PL and **ind-mask**. It can be seen that compared to independent update, the cooperation among agents can fasten the convergence rate and improve the model accuracy, showing the effectiveness of the designed algorithm. Then we compare the two independent methods **ind-mask** and **ind-weipru**. In the early iterations, **ind-mask** has slower convergence rate, while its eventual accuracy is higher than **ind-weipru**. It is resulted from the model pruning in **ind-weipru**. Finally, the partially averaging method **par-weipru** performs better than **avr-weipru**, due to

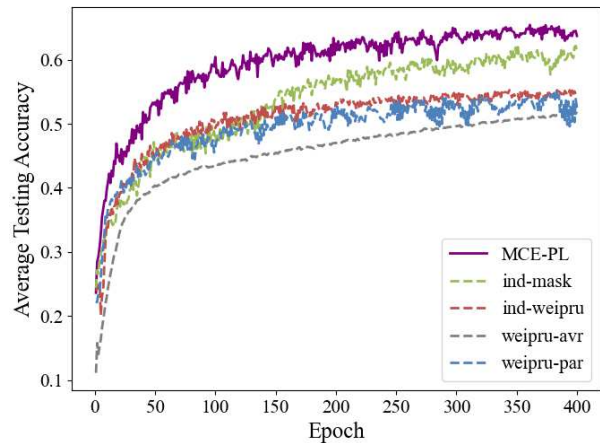


Fig. 6: The convergence curves of different algorithms.

the heterogeneity among agents. However, it performs worse than **ind-weipru**, showing its limited effectiveness in such highly heterogeneous scenarios. Compared to these baseline algorithms, the proposed MCE-PL has the fastest convergence rate and the highest test accuracy.

We also compared the proposed MCE-PL with Dis-PFL [24] to evaluate its performance. The model testing accuracy of these algorithms under different number of local labels $c_i = 3, 4, 5$, as shown in Table. II. It can be seen that the proposed MCE-PL outperforms the other baseline methods in this label distribution skew condition. With the increase of c_i , the advantages of MCE-PL become more significant and the cooperation can be more effective, due to the enhanced relativities of data distributions among agents.

TABLE II: The comparison of averaged testing accuracy among different algorithms under data and node heterogeneity.

	$c_i = 3$	$c_i = 4$	$c_i = 5$
MCE-PL	0.7088	0.6451	0.5759
ind-mask	0.6808	0.6140	0.5413
ind-weipru	0.6239	0.5484	0.4813
weipru-avr	0.5515	0.5187	0.4564
weipru-par	0.6068	0.5251	0.4643
Dis-PFL	0.5742	0.5609	0.5617

Finally, we show the communication cost curves of the collaborative methods, MCE-PL, **avr-weipru** and **par-weipru**. Under the same simulation settings as above with $c_i = 4$, the communication cost is measured by the amount of data transmitted. For **avr-weipru** and **par-weipru** based on real-valued parameters, the size of each transmission package is equal to the number of the parameters, where each data is a 32 bit float. For MCE-PL, the size of each binary data is 1 bit. Then we get the curves of test accuracy with the communication cost in Fig. 7.

It can be observed from Fig. 7 that the proposed MCE-PL has much less communication cost compared with weipru-avr and weipru-par based on real-valued parameters. Additionally, Dis-PFL has higher communication costs due to the transmission of both the pruned model and binary masks, while the mask-growing technique in Dis-DFL results in a

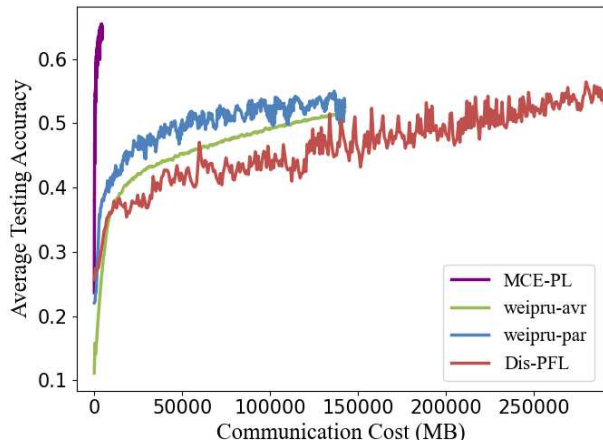


Fig. 7: The comparison of communication cost.

denser model than the intended sparsity. Furthermore, MCE-PL achieves higher accuracy at the same communication cost, demonstrating its communication efficiency.

D. Comparison of Learned Model

Then given the above simulation settings, following we show the comparison of the learned models in MCE-PL and **ind-mask**. Specifically, consider node 2, 4, 6, 8 whose model retention ratios are 0.4, 0.2, 0.1, 0.2 respectively. For the first convolutional layer with size $3 \times 64 \times 5 \times 5$ in each agent, we plot part of the learned model, to display the results more clearly and concisely. We select the middle 20 filters and the convolutional kernels with size $3 \times 20 \times 5 \times 5$ are shown in Fig. 8 and Fig. 9. The horizontal axis is the output dimension while the vertical axis is the input dimension, with each kernel of size 5×5 . To better compare the learned models in different agents under same r_i , the results are shown in the order of Agent 2, 4, 8, 6. Moreover, we select two filters and zoom in for a better comparison between agent 4 and agent 8, to show their difference in each kernel.

Firstly, it can be observed in Fig. 8 that MCE-PL algorithm learns heterogeneous models among agents. The model retention ratios for nodes 2, 4, 6 are 0.4, 0.2, 0.1 respectively. Correspondingly, it can be observed in Fig. 8 that the sparsity of the learned model becomes larger and the number of non-zero entries becomes smaller. This validates the effectiveness of MCE-PL in node heterogeneity. Secondly, $r_i = 0.2$ for both node 4 and 8. Compare the learned models of MCE-PL between the two nodes especially shown in the right of Fig. 8, certain differences exist between the two partial models. For the 5 convolutional kernels which are not total zero, the non-zero entries in the two models are different as compared within the blue box. For the output dimension, the fifth to last filter of node 8 is not exactly zero, while that of node 4 is all zero as compared within the red box. These differences mainly come from the statistical heterogeneity between the two nodes, validating the effectiveness of MCE-PL for data heterogeneity. To sum up, the proposed MCE-PL can effectively conduct personalized learning in both data and node heterogeneous conditions.

Then we compare the learned models of the two algorithms in Fig. 8 and Fig. 9. It can be observed the independent updating algorithm **ind-mask** has more sparsity in the output dimension. Take node 4 for example. The number of non-zero output dimensions in the selected partial model is 7 in MCE-PL and 3 in **ind-mask**. Such phenomenon mainly comes from the information aggregation procedure in MCE-PL, where the neighboring heterogeneous models have an impact on the local model and the non-zero entries cannot concentrate on only few output dimensions. Such impact may revise the local model and improve the accuracy while reducing the sparsity to some extent. Moreover, as shown in the blue boxes in Fig. 8 and 9, the difference between learned models is much smaller in MCE-PL compared with that in **ind-mask**, which is resulted from the collaboration among agents in MCE-PL while the **ind-mask** conducts independent training. It should be noted that there may exist multiple binary mask tensors that can achieve good performance due to the non-convexity of the problem. In the independent training and without any constraint, the learned subnetworks among agents may share less correlation as shown in Fig. 9. On the other hand, the cooperation among agents in MCE-PL equivalently poses the constraint on the subnetworks, which show more similarity.

E. Different Communication Network Topologies

In this section, we provide a comprehensive evaluation of the proposed MCE-PL across different communication network topologies. Specifically, we evaluate its testing accuracy under different connectivity probabilities among agents, denoted by p , and also consider an extreme case of ring topology. The results, presented in Table III, show that MCE-PL performs well regardless of the communication network topology, further validating its generalization capability.

TABLE III: The comparison of averaged testing accuracy under different connectivity probability among agents.

	ring	$p = 0.3$	$p = 0.5$	$p = 0.7$
MCE-PL	0.6394	0.6489	0.6451	0.6476

VI. CONCLUSION

This paper proposed a communication-efficient personalized learning algorithm considering both statistical and system heterogeneity, named as MCE-PL. Based on the proposed distributed strong lottery ticket hypothesis, the global real-valued parameters for each agent are initialized and fixed, while each local model is pruned by updating binary mask tensor. To leverage the relationship among agents, each agent's binary mask tensor was transmitted to its neighboring nodes. We designed an aggregation procedure incorporating an aggregation tensor and a personalized fine-tuning step. Finally, we compared the performance of MCE-PL with existing methods designed for heterogeneous conditions. The experimental results validate the superiority of the proposed algorithm.

In real-world IoT environments with limited bandwidth and computational constraints, the proposed method is well-adapted with the binary information transmission and heterogeneous pruning ratio, corresponding to computational

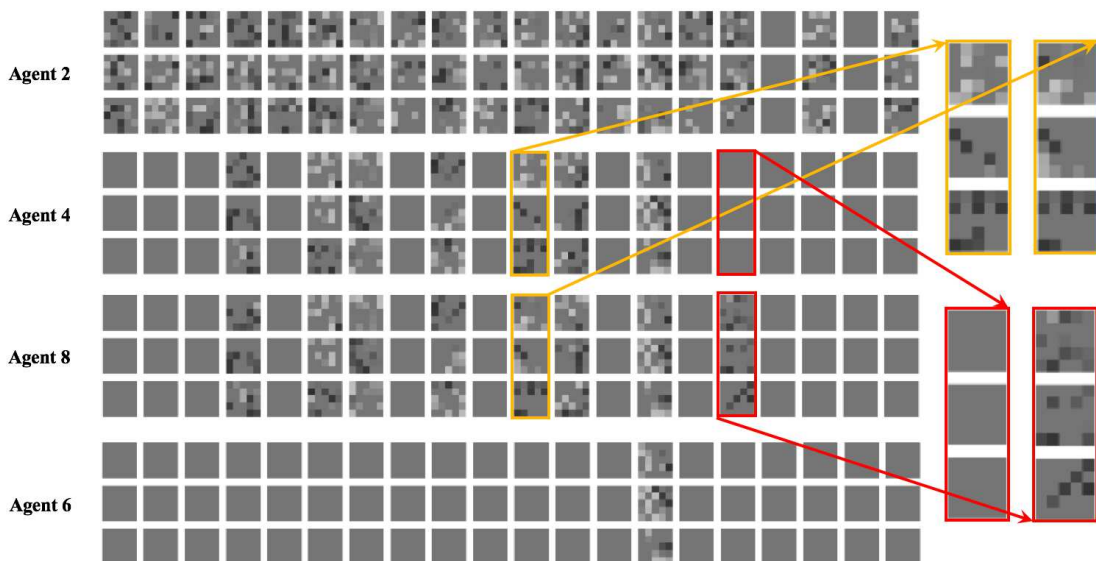


Fig. 8: The learned personalized models in different agents by MCE-PL.

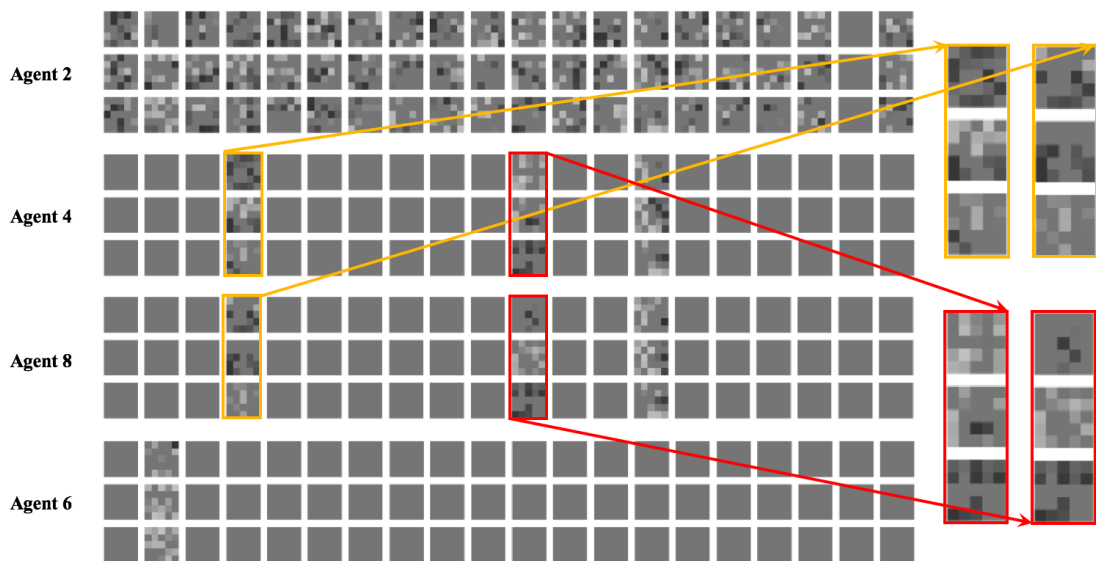


Fig. 9: The learned personalized models in different agents by **ind-mask**.

constraints. Moreover, due to small communication cost and the aggregation procedure only relying on neighboring nodes, MCE-PL has great scalability for large-scale deployments. There are still several open research topics. One of them is to consider heterogeneous models with different depth. Additionally, in practical communication networks, the model retention ratio for each agent cannot be assumed to be known in advance; it needs to be estimated by solving an optimization problem that considers factors like latency or load balancing, while also accounting for the capabilities of each agent.

APPENDIX A PROOF OF THEOREM 1

By (22) in Lemma 1, it can be easily known that there exist \mathbf{m}_1 and \mathbf{m}_2 such that the following local properties hold at the same time with probability $(1 - \delta)^2$:

$$\sup_{\mathbf{x} \in \mathcal{X}} \|f_1(\mathbf{x}) - g_{\mathbf{m}_1}(\mathbf{x})\|_{\max} \leq \varepsilon_1,$$

$$\sup_{\mathbf{x} \in \mathcal{X}} \|f_2(\mathbf{x}) - g_{\mathbf{m}_2}(\mathbf{x})\|_{\max} \leq \varepsilon_2. \quad (\text{A.1})$$

According to the definition of $\|\cdot\|_{\max}$, we have

$$\sup_{\mathbf{x} \in \mathcal{X}} \|f_1(\mathbf{x}) - f_2(\mathbf{x}) - [g_{\mathbf{m}_1}(\mathbf{x}) - g_{\mathbf{m}_2}(\mathbf{x})]\|_{\max} \leq \varepsilon_1 + \varepsilon_2. \quad (\text{A.2})$$

By Assumption 3, we have

$$\sup_{\mathbf{x} \in \mathcal{X}} \|f_1(\mathbf{x}) - f_2(\mathbf{x})\|_{\max} \leq \alpha_u, \quad (\text{A.3})$$

$$\inf_{\mathbf{x} \in \mathcal{X}} \|f_1(\mathbf{x}) - f_2(\mathbf{x})\|_{\max} \geq \alpha_l. \quad (\text{A.4})$$

$$\inf_{\mathbf{x} \in \mathcal{X}} \|f_1(\mathbf{x}) - f_2(\mathbf{x}) - [g_{\mathbf{m}_1}(\mathbf{x}) - g_{\mathbf{m}_2}(\mathbf{x})]\|_{\max} \geq 0. \quad (\text{A.5})$$

By combining (A.2) and (A.3), we have

$$\sup_{\mathbf{x} \in \mathcal{X}} \|g_{\mathbf{m}_1}(\mathbf{x}) - g_{\mathbf{m}_2}(\mathbf{x})\|_{\max} \leq \varepsilon_1 + \varepsilon_2 + \alpha_u. \quad (\text{A.6})$$

Then, by combining (A.4), (A.5), (A.6), we have

$$\inf_{\mathbf{x} \in \mathcal{X}} \|g_{\mathbf{m}_1}(\mathbf{x}) - g_{\mathbf{m}_2}(\mathbf{x})\|_{\max}$$

$$\geq \min\{|\varepsilon_1 + \varepsilon_2 - \alpha_l|, |\varepsilon_1 + \varepsilon_2 - \alpha_u|, |\alpha_l|\}. \quad (\text{A.7})$$

This completes the proof. ■

REFERENCES

- [1] Y. Li, S. Wang, C.-Y. Chi, and T. Q. S. Quek, "Differentially private federated clustering over non-iid data," *IEEE Internet of Things Journal*, vol. 11, no. 4, pp. 6705–6721, 2024.
- [2] Z. Tian, Z. Zhang, and L. Hanzo, "Distributed Multi-View Sparse Vector Recovery," *IEEE Trans. Signal Process.*, vol. 71, pp. 1448–1463, 2023.
- [3] Z. Tian, Z. Zhang, Z. Yang, R. Jin and H. Dai, "Distributed Learning Over Networks With Graph-Attention-Based Personalization," *IEEE Trans. Signal Process.*, vol. 71, pp. 2071–2086, 2023.
- [4] X. Lian, C. Zhang, H. Zhang, C. Hsieh, W. Zhang, and J. Liu, "Can decentralized algorithms outperform centralized algorithms? A case study for decentralized parallel stochastic gradient descent," in *Proc. Adv. Neural Inf. Process. Syst. (NIPS)*, pp. 5330–5340, 2017.
- [5] A. Fallah, A. Mokhtari, and A. E. Ozdaglar, "Personalized federated learning with theoretical guarantees: A model-agnostic meta-learning approach," in *Proc. Adv. Neural Inf. Process. Syst. (NIPS)*, pp. 3557–3568, 2020.
- [6] D. Caldarola, M. Mancini, F. Galasso, M. Ciccone, E. Rodola, and B. Caputo, "Cluster-driven graph federated learning over multiple domains," in *Proc. IEEE Conf. Comput. Vis. Pattern Recognit. (CVPR) Workshops*, pp. 2743–2752, 2021.
- [7] T. Li, A. K. Sahu, M. Zaheer, M. Sanjabi, A. Talwalkar, and V. Smith, "Federated optimization in heterogeneous networks," in *Proc. Machine learning and systems*, vol. 2, pp. 429–450, 2020.
- [8] A. Ghosh, J. Chung, D. Yin, and K. Ramchandran, "An efficient framework for clustered federated learning," in *Proc. Adv. Neural Inf. Process. Syst. (NIPS)*, pp. 19586–19597, 2020.
- [9] C. T. Dinh, N. Tran, and J. Nguyen, "Personalized federated learning with moreau envelopes," in *Proc. Adv. Neural Inf. Process. Syst. (NIPS)*, pp. 21394–21405, 2020.
- [10] C. He, M. Annavaram and S. Avestimehr, "Group knowledge transfer: Federated learning of large cnns at the edge," in *Proc. Adv. Neural Inf. Process. Syst. (NIPS)*, pp. 14068–14080, 2020.
- [11] O. Gupta and R. Raskar, "Distributed learning of deep neural network over multiple agents," in *Jour. Network and Computer Applications*, vol. 116, pp. 1–8, 2018.
- [12] E. Diao, J. Ding, and V. Tarokh, "Heterofl: Computation and communication efficient federated learning for heterogeneous clients," *arXiv: 2010.01264*, 2020.
- [13] S. Horvath, S. Laskaridis, M. Almeida, I. Leontiadis, S. Venieris and N. Lane, "Fjord: Fair and accurate federated learning under heterogeneous targets with ordered dropout," in *Proc. Adv. Neural Inf. Process. Syst. (NIPS)*, pp. 12876–12889, 2021.
- [14] Y. Deng, W. Chen, J. Ren, F. Lyu, Y. Liu, Y. Liu and Y. Zhao, "Fjord: Fair and accurate federated learning under heterogeneous targets with ordered dropout," in *Proc. Adv. Neural Inf. Process. Syst. (NIPS)*, pp. 12876–12889, 2021.
- [15] A. Li, J. Sun, B. Wang, L. Duan, S. Li, Y. Chen, and H. Li, "Lotteryfl: Personalized and communication-efficient federated learning with lottery ticket hypothesis on non-iid datasets," *arXiv: 2008.03371*, 2020.
- [16] S. Seo, S. W. Ko, J. Park, S. L. Kim, and M. Bennis, "Communication-efficient and personalized federated lottery ticket learning," in *2021 IEEE 22nd Int. Workshop Signal Process. Advances in Wireless Communications (SPAWC)*, pp. 581–585, Sep. 2021.
- [17] Y. Jiang, S. Wang, V. Valls, B. J. Ko, W. H. Lee, K. K. Leung, and L. Tassiulas, "Model pruning enables efficient federated learning on edge devices," in *IEEE Trans. Neural Networks and Learning Systems*, vol. 34, no. 12, pp. 10374–10386, 2022.
- [18] D. Yao, W. Pan, M. J. O'Neill, Y. Dai, Y. Wan, H. Jin, and L. Sun, "Fedhm: Efficient federated learning for heterogeneous models via low-rank factorization," *arXiv: 2111.14655*, 2021.
- [19] Y. Niu, S. Prakash, S. Kundu, S. Lee, and S. Avestimehr, "Federated learning of large models at the edge via principal sub-model training," *arXiv: 2208.13141*, 2022.
- [20] Y. Mei, P. Guo, M. Zhou and V. Patel, "Resource-adaptive federated learning with all-in-one neural composition," in *Proc. Adv. Neural Inf. Process. Syst. (NIPS)*, pp. 4270–4284, 2022.
- [21] V. Zantedeschi, A. Bellet and M. Tommasi, "Fully decentralized joint learning of personalized models and collaboration graphs," in *International Conf. Artif. Intell. Statist.*, pp. 864–874, 2020.
- [22] S. Chen, Y. Xu, H. Xu, Z. Ma and Z. Wang, "Enhancing Decentralized and Personalized Federated Learning with Topology Construction," in *IEEE Trans. Mobile Computing*, pp. 1–16, 2024.
- [23] G. Xiong, G. Yan, S. Wang, Z. Ma and J. Li, "DePRL: Achieving Linear Convergence Speedup in Personalized Decentralized Learning with Shared Representations," in *Proc. AAAI Conf. Artif. Intell.*, vol. 38, pp. 16103–16111, 2024.
- [24] R. Dai, L. Shen, F. He, X. Tian and D. Tao, "Dispf: Towards communication-efficient personalized federated learning via decentralized sparse training," in *Int. Conf. Mach. Learning*, pp. 4587–4604, 2022.
- [25] R. Hong and A. Chandra, "Dlion: Decentralized distributed deep learning in micro-clouds," in *Proc. 30th Int. Symposium on High-Performance Parallel and Distributed Computing*, pp. 227–238, 2021.
- [26] D. Yang, W. Rang, and D. Cheng, "Mitigating stragglers in the decentralized training on heterogeneous clusters," in *Proc. 21st Int. Middleware Conf.*, pp. 386–399, 2020.
- [27] K. Yang, T. Jiang, Y. Shi, and Z. Ding, "Federated learning via over-the-air computation," in *IEEE Trans. Wireless Commun.*, vol. 19, no. 3, pp. 2022–2035, 2020.
- [28] S. Wang, T. Tuor, T. Salonidis, K. K. Leung, C. Makaya, T. He and K. Chan, "Adaptive federated learning in resource constrained edge computing systems," in *IEEE Jour. Selected Areas Commun.*, vol. 37, no. 6, pp. 1205–1221, 2019.
- [29] C. Li, G. Li, and P. K. Varshney, "Communication-efficient federated learning based on compressed sensing," in *IEEE Internet of Things Journal*, vol. 8, no. 20, pp. 15531–15541, 2021.
- [30] Y. Li, C.-W. Huang, S. Wang, C.-Y. Chi, and T. Q. Quek, "Privacy-preserving federated primal-dual learning for non-convex and non-smooth problems with model sparsification," in *IEEE Internet of Things Journal*, vol. 11, no. 15, pp. 25853–25866, 2024.
- [31] M. Doostmohammadian, Z. R. Gabidullina, and H. R. Rabiee, "Nonlinear perturbation-based non-convex optimization over time-varying networks," in *IEEE Trans. Network Science and Engineering*, 2024.
- [32] M. Doostmohammadian, M. I. Qureshi, M. H. Khalesi, H. R. Rabiee, and U. A. Khan, "Log-Scale Quantization in Distributed First-Order Methods: Gradient-based Learning from Distributed Data," in *IEEE Trans. Automation Science and Engineering*, 2025.
- [33] A. Li, J. Sun, X. Zeng, M. Zhang, H. Li and Y. Chen, "Fedmask: Joint computation and communication-efficient personalized federated learning via heterogeneous masking," in *Proc. 19th ACM Conf. Embedded Networked Sensor Systems*, pp. 42–55, 2021.
- [34] R. Fotohi, F. S. Aliee and B. Farahani, "A lightweight and secure deep learning model for privacy-preserving federated learning in intelligent enterprises," *IEEE Internet of Things Journal*, 2024.
- [35] R. Fotohi, F. S. Aliee and B. Farahani, "Decentralized and robust privacy-preserving model using blockchain-enabled federated deep learning in intelligent enterprises," *Applied Soft Computing*, vol. 161, 2024.
- [36] H. Zhou, J. Lan, R. Liu and J. Yosinski, "Deconstructing lottery tickets: Zeros, signs, and the supermask," in *Proc. Adv. Neural Inf. Process. Syst. (NIPS)*, vol. 32, 2019.

- [37] E. Malach, G. Yehudai, S. Shalev-Schwartz, and O. Shamir, “Proving the lottery ticket hypothesis: Pruning is all you need,” in *Int. Conf. Mach. Learning*, pp. 6682–6691, 2020.
- [38] J. Frankle, and M. Carbin, “The Lottery Ticket Hypothesis: Finding Sparse, Trainable Neural Networks,” in *Int. Conf. Learning Represent.*, 2018.
- [39] V. Ramanujan, M. Wortsman, A. Kembhavi, A. Farhadi, and M. Rastegari, “What’s hidden in a randomly weighted neural network?,” in *Proc. IEEE Conf. Comput. Vis. Pattern Recognit. (CVPR)*, pp. 11893–11902, 2020.
- [40] A. Pensia, S. Rajput, A. Nagle, H. Vishwakarma, and D. Papailiopoulos, “Optimal lottery tickets via subset sum: Logarithmic over-parameterization is sufficient,” in *Proc. Adv. Neural Inf. Process. Syst. (NIPS)*, vol. 33, pp. 2599–2610, 2020.
- [41] A. da Cunha, E. Natale, and L. Viennot, “Proving the strong lottery ticket hypothesis for convolutional neural networks,” in *Int. Conf. Learning Represent.*, 2022.
- [42] S. Scardapane, D. Comminiello, A. Hussain, and A. Uncini, “Group sparse regularization for deep neural networks,” in *Neurocomputing*, vol. 241, pp. 81–89, 2017.
- [43] K. Mitsuno, J. Miyao, and T. Kurita, “Hierarchical group sparse regularization for deep convolutional neural networks,” in *2020 Int Joint Conf. Neural Networks (IJCNN)*, pp. 1–8, 2020.